Rotation dependence of electric quadrupole hyperfine interaction in the ground state of molecular iodine by high-resolution laser spectroscopy

Feng-Lei Hong,* Jun Ye, Long-Sheng Ma,† Susanne Picard,‡ Christian J. Bordé,¶ and John L. Hall****

JILA, National Institute of Standards and Technology, and University of Colorado, Boulder, Colorado 80309-0440

Received June 12, 2000; revised manuscript received October 17, 2000

Doppler-free high-resolution spectroscopy is applied to molecular iodine at 532 nm by Nd:YAG lasers. The main hyperfine components as well as the crossover lines are measured for $R(56)32\text{-}0$ and $P(54)32\text{-}0$ transitions by heterodyne beating of two I_2-stabilized lasers. The measured hyperfine splittings including both main and crossover lines are fitted to a four-term Hamiltonian, which includes the electric quadrupole, spin–rotation, tensor spin–spin, and scalar spin–spin interactions, with an average deviation of ~1 kHz. Absolute values of the electric quadrupole hyperfine constants for both the upper and the lower states are obtained. The rotation dependence of the ground-state ($v'' = 0$) electric quadrupole constant eQq'' is found to be $eQq''(J) = -2452.556(2) - 0.000164(5)J(J+1) - 0.000000005(2)J^2(J+1)^2$ MHz. © 2001 Optical Society of America

OCIS codes: 020.2930, 300.6320, 300.6390, 120.3940, 300.6460.

1. INTRODUCTION

Molecular iodine (I_2) has always been an attractive subject for spectroscopy because of its rich spectra from the UV to the IR. Hyperfine interactions in I_2 have been studied extensively in the past two decades, yielding increasing resolution and accuracy. The hyperfine splitting of iodine lines has been measured by Doppler-free laser spectroscopy with argon-ion lasers,[1–3] krypton-ion lasers,[1] He-Ne lasers,[4–6] and dye lasers.[7] A tabulation of the hyperfine structures in $^{127}I_2$ can be found in Ref. 8. Recent research has increased the accuracy with which iodine can serve as wavelength and frequency references.

Recently, diode-pumped Nd:YAG lasers were recognized as promising sources for high-resolution spectroscopy because of their inherently low-frequency noise, high power, and high reliability. By locking of second-harmonic generation (SHG) of the Nd:YAG lasers to hyperfine lines of I_2 at 532 nm, lasers at JILA have reached the Allan frequency stability of 5×10^{-14} at 1 s, improving after 100 s to $\sim 5 \times 10^{-15}$.[9,13] The hyperfine splittings of iodine lines near 532 nm have been measured at Stanford University[10,11] and at JILA.[12,13]

The hyperfine spectrum of iodine is important for metrological applications. One of the most popular ways to establish a realization of the Metre is to use a 633-nm He–Ne laser that is frequency locked onto one of the hyperfine lines of I_2. Furthermore, six of the twelve radiation values recommended for realization of the Metre are obtained from iodine-stabilized lasers.[14] The absolute optical frequency of hyperfine component a_{10} in the $R(56)32\text{-}0$ transition at 532 nm has been measured at JILA,[9,15,16] and frequency comparisons of I_2-stabilized Nd:YAG lasers have been carried out internationally.[17,18] I_2-stabilized lasers are also used as frequency standards for precision spectroscopic measurements and accurate determination of physical constants.

I_2 also provides a good subject with which to test theoretical models of hyperfine interactions. The Hamiltonian of the hyperfine interactions, H_{hfs}, can be written as[2,3]

$$H_{\mathrm{hfs}} = eQq \times H_{\mathrm{EQ}} + C \times H_{\mathrm{SR}} + d \times H_{\mathrm{TSS}} + \delta \times H_{\mathrm{SSS}}, \tag{1}$$

where H_{EQ}, H_{SR}, H_{TSS}, and H_{SSS} represent, respectively, the electric quadrupole, spin–rotation, tensor spin–spin, and scalar spin–spin interactions and eQq, C, d, and δ represent the corresponding hyperfine constant for each of these interactions. Because the selection rules of the main rovibrational transitions between the X (ground) and the B (excited) electronic states are very strict ($\Delta F = \Delta J$, $\Delta J = \pm 1$), the hyperfine splitting patterns are nearly identical to those of either the initial or the final state, except that the splittings are scaled by the differences between the hyperfine constants in the two states. In other words, in these main transitions the hyperfine structure quantum numbers remain unchanged, whereas only the hyperfine coupling constants change. The differences in the hyperfine constants between the excited and the ground states are written as

$$\begin{aligned} \Delta(eQq) &= eQq' - eQq'', \\ \Delta C &= C' - C'', \\ \Delta d &= d' - d'', \\ \Delta\delta &= \delta' - \delta''. \end{aligned} \tag{2}$$

0740-3224/2001/030379-09$15.00

By fitting the observed spectra of the main transitions to the theoretical expectations represented by Eq. (1), one can obtain accurate values for $\Delta(eQq)$, ΔC, Δd, and $\Delta\delta$ but only a crude estimate of the absolute values for the respective ground and excited states. However, by observing also the so-called crossover transitions between the main lines ($\Delta F = \Delta J$) and the much weaker forbidden transitions ($\Delta F = 0$), one can determine accurately the absolute values of the hyperfine constants for both the upper and the lower states. In the pioneering research, the ground state eQq'' for $v'' = 0$ and $J'' = 13$ was measured by this method and found to be -2452 ± 40 MHz.[19]

Using measurements made by the molecular-beam magnetic resonance method, Yokozeki and Muenter measured and calculated the four hyperfine constants of the ground state ($v'' = 0$ and $J'' = 13$) with good precision.[20] Their values, $eQq'' = -2\,452\,583.7(16)$ kHz, $C'' = 3.162(8)$ kHz, $d'' = 1.58(5)$ kHz, and $\delta'' = 3.66(3)$ kHz, have been used in many subsequent calculations[10–13] to represent the lower state and thus to allow one to obtain the hyperfine constants for the excited states. (Here we use the convention that the standard uncertainty in parentheses applies to the last digit of the value.) However, the quoted hyperfine-constant values give only a close approximation in those calculations because different rotational states are involved, albeit in the same vibrational ground state. The question is: Is there measurable rotational dependence for those hyperfine constants of the ground state with $v'' = 0$? Recently, Bordé and his colleagues[21,22] measured the hyperfine splittings in the ground state for $J'' = 13$ and $J'' = 15$ rotational levels by using stimulated Raman spectroscopy and derived hyperfine constants with higher accuracy than those described in Ref. 20. Within the experimental precision, they found that the constants were identical for both rotational levels, except for quadrupole coupling constants eQq'', which differed from $J'' = 13$ and $J'' = 15$.

We measured both main and crossover lines for the $R(56)32\text{-}0$ and $P(54)32\text{-}0$ transitions by using modulation transfer spectroscopy.[23–25] Both main and crossover lines were fitted to the four-term Hamiltonian as shown in Eq. (1). From this, absolute values of the hyperfine constants of the upper and lower levels for both $J'' = 56$ and $J'' = 54$ transitions were derived.

With the high signal-to-noise (S/N) ratio achieved in the JILA iodine spectrometer and the high stability and accuracy attained as a consequence,[9,12,13] we could fit the observed results including both main and crossover lines to the four-term Hamiltonian with ~1-kHz uncertainty. From the fitting, we could also observe various eQq'' values for the ground states with different J numbers. Combining our values with the eQq'' values from Ref. 21, we obtained a formula for the rotation dependence of the ground state eQq''.

2. EXPERIMENT

A. Experimental Setup

Figure 1 shows a block diagram of our measurement system. The optical part of the system contains a source laser oscillator, a buildup cavity for SHG, and an iodine spectrometer. The source oscillator of each system is a commercial diode-pumped Nd:YAG laser, which has a nonplanar ring resonator formed in the monolithic gain medium. SHG of each system is accomplished through an external ring buildup cavity with an intracavity nonlinear crystal, either $KNbO_3$ or $MgO{:}LiNbO_3$. The SHG cavities are locked to the source oscillators by either a dither method[12] or a polarization method.[23]

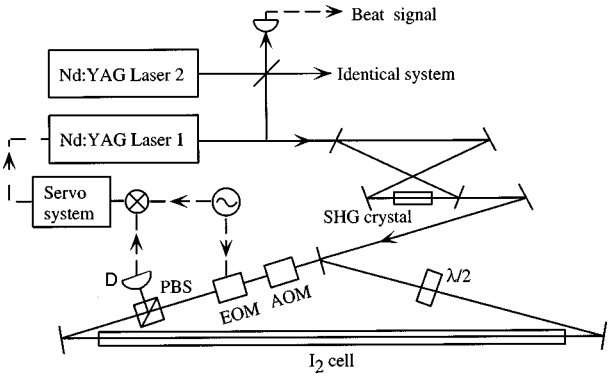

Fig. 1. Diagram of the experimental setup: D, detector; other abbreviations defined in text.

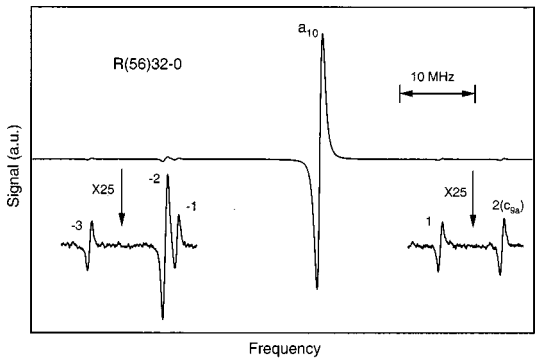

Fig. 2. Observed main hyperfine component a_{10} of the $R(56)32\text{-}0$ transition and the crossover lines nearby. The crossover lines are numbered in series as -1, -2, -3,... if the frequency is lower than that of the a_{10} component and as 1, 2,... if the frequency is higher than that of a_{10}. Crossover line 2, numbered c_{9a}, is included in the calculation.

The spectroscopy of molecular iodine is based on the sub-Doppler technique of modulation transfer,[24–26] which gives a nearly flat baseline and is therefore quite attractive for laser spectroscopy and frequency stabilization. As shown in Fig. 1, the green beam from the SHG cavity is divided, by an appropriate beam splitter, into a strong pump beam and a weak probe beam in the iodine spectrometer. The pump beam is frequency shifted by an acousto-optic modulator (AOM) and is phase modulated by an electro-optic modulator (EOM). The AOM works as an optical isolator to prevent interferometric noise in the spectrometer. To further reduce the interference between the linearly polarized pump and probe beams, we rotate the polarization of the probe beam with a λ/2 plate to be orthogonal to that of the pump beam. The probe beam, separated by a polarization beam splitter (PBS), reaches a detector after interacting with the pump beam inside the 1.2-m-long iodine cell. The unmodulated probe beam passes through the iodine cell and, as a result of nonlinear four-wave mixing with the modulated pump

beam, develops new sidebands. Beat currents at the modulation frequency are generated in the photodetector between the new sidebands and the laser carrier. This signal is demodulated by a double-balanced mixer and used to control the laser frequency through a servo system.

Two independent systems were built in which each laser frequency is doubled and locked to its own iodine cell. The heterodyne beat frequency between the two lasers is measured at 1064 nm (IR light) by an avalanche photodetector. All the measured frequency intervals (in the IR) described in this paper have been multiplied by a factor of 2, corresponding to correct interval values at 532 nm. More-detailed descriptions of the systems are given elsewhere.[12,13]

B. Observation of Main and Crossover Hyperfine Transitions

Figure 2 shows the observed modulation transfer signal of the a_{10} hyperfine component of the $R(56)32\text{-}0$ transition and the crossover lines nearby. The EOM worked at a modulation frequency of 350 kHz with a modulation index of ~0.9. The AOM was driven by an 80-MHz rf source. The cold-finger temperature of the iodine cell was held at −15 °C, corresponding to an iodine-vapor pressure of 0.787 Pa. The pump power was 7.6 mW, and the probe power was 0.4 mW. As discussed in Ref. 13, although the crossover resonances are $\sim 1/(2J)$ less intense than the main lines, they will increase in size much faster than the main lines when the input optical power is increased in the saturation spectrometer. This is so simply because the main lines have already been operated in the saturation regime, whereas the crossover can still grow linearly as a result of the unsaturated $\Delta F = 0$ transitions.

We also present the crossover lines in Fig. 2 by expanding the signal size 25 times vertically. The S/N ratio for the crossover lines is ~100 in a 32-Hz bandwidth (5-ms time constant). The crossover lines are numbered in series here as −1, −2, −3,... if their frequencies are lower than that of the a_{10} component and are numbered as 1,

Table 1. Observed and Calculated Hyperfine Components of $R(56)32\text{-}0$[a]

Hyperfine Components	Observed (kHz)	Calculated (kHz)	Obs. − Cal. (kHz)	Weight	Total Angular Momentum (F)	Total Nuclear Spin (I)
Main						
a_1	0	0	0	10.0	57	2
a_2	259 697.4	259 696.6	0.8	10.0	53	4
a_5	311 366.8	311 366.6	0.2	10.0	61	4
a_6	401 477.5	401 478.3	−0.7	10.0	54	4
a_7	416 993.1	416 994.0	−0.9	10.0	55	4
a_8	439 626.5	439 626.7	−0.2	10.0	59	4
a_9	455 343.2	455 343.8	−0.6	10.0	60	4
a_{10}	571 541.8	571 541.3	0.5	10.0	57	4
a_{11}	698 054.2	698 054.6	−0.4	10.0	55	2
a_{12}	702 754.1	702 753.2	0.9	10.0	56	4
a_{13}	726 030.5	726 029.9	0.6	10.0	58	4
a_{14}	732 207.1	732 207.3	−0.2	10.0	59	2
a_{15}	857 953.7	857 953.8	−0.1	10.0	57	0
Crossover					Common Level	
c_{1a}	180 446.2	180 448.5	−2.3	1.0	Upper	
c_{2a}	241 268.5	241 265.6	2.9	1.0	Lower	
c_{3a}	329 445.1	329 448.2	−3.1	1.0	Upper	
c_{4a}	347 630.6	347 628.2	2.4	1.0	Upper	
c_{5a}	359 414.5	359 416.6	−2.1	1.0	Upper	
c_{6a}	381 364.7	381 363.8	0.9	1.0	Upper	
c_{7a}	384 282.6	384 281.4	1.2	1.0	Upper	
c_{8a}	446 451.4	446 448.7	2.7	1.0	Upper	
c_{9a}	597 525.2	597 526.0	−0.8	1.0	Upper	
c_{10a}	609 179.0	609 177.1	1.9	1.0	Lower	
c_{11a}	614 970.6	614 973.0	−2.4	1.0	Upper	
c_{12a}	667 603.5	667 606.5	−3.0	1.0	Upper	
c_{13a}	769 967.2	769 968.0	−0.8	1.0	Upper	
c_{14a}	799 024.4	799 024.0	0.4	1.0	Upper	
c_{15a}	876 626.1	876 624.3	1.8	1.0	Lower	

[a] The standard deviation of the fit, including both main and crossover lines, is 0.95 kHz.

Table 2. Observed and Calculated Hyperfine Components of $P(54)32\text{-}0^a$

Hyperfine Components	Observed (kHz)	Calculated (kHz)	Obs. − Cal. (kHz)	Weight	Total Angular Momentum (F)	Total Nuclear Spin (I)
Main						
a_1	0	0	0	10.0	53	2
a_2	260 992.4[b]	260 992.0	0.4	10.0	49	4
a_3	285 007.7[b]	285 008.3	−0.6	10.0	54	2
a_4	286 726.4[b]	286 726.1	0.3	10.0	52	2
a_5	310 066.4[b]	310 066.6	−0.2	10.0	57	4
a_6	402 249.5[b]	402 250.2	−0.7	10.0	50	4
a_7	417 667.7[b]	417 668.0	−0.3	10.0	51	4
a_8	438 918.6[b]	438 918.2	0.4	10.0	55	4
a_9	454 563.4[b]	454 563.4	0.0	10.0	56	4
a_{10}	571 536.4[b]	571 535.6	0.8	10.0	53	4
a_{11}	698 613.6[b]	698 613.6	0.0	10.0	51	2
a_{12}	702 934.8[b]	702 934.5	0.3	10.0	52	4
a_{13}	725 833.9[b]	725 833.5	0.4	10.0	54	4
a_{14}	731 687.9[b]	731 688.0	−0.1	10.0	55	2
a_{15}	857 960.8[b]	857 960.9	−0.1	10.0	53	0
Crossover					Common Level	
c_{1a}	−37 820.4	−37 827.0	6.6	1.0	Lower	
c_{2a}	342 911.6	342 916.7	−5.1	1.0	Upper	
c_{3a}	374 079.4	374 077.8	1.6	1.0	Upper	
c_{4a}	478 368.0	478 363.5	4.5	1.0	Lower	
c_{5a}	629 601.2	629 605.8	−4.6	1.0	Upper	
c_{6a}	659 140.7	659 139.5	1.2	1.0	Upper	
c_{7a}	813 656.2	813 659.2	−3.0	1.0	Upper	
c_{8a}	879 721.1	879 722.8	−1.7	1.0	Lower	

[a] The standard deviation of the fit including both main and crossover lines is 1.13 kHz.
[b] The frequency values of the observed main lines were published in Ref. 13.

Table 3. Fitted Hyperfine Constants

Parameter	$R(56)32\text{-}0$	$P(54)32\text{-}0$	$R(15)43\text{-}0^a$	$P(13)43\text{-}0^a$
eQq'' (MHz)	−2453.132(11)	−2453.088(24)	−2452.59699(45)	−2452.58514(45)
C'' (kHz)	3.306(21)	2.904(40)	3.1543(29)	3.1536(33)
d'' (kHz)	1.524[b]	1.524[b]	1.519(18)	1.528(18)
δ'' (kHz)	3.705[b]	3.705[b]	3.701(23)	3.708(22)
eQq' (MHz)	−544.751(11)	−544.656(24)	–	–
C' (kHz)	89.656(21)	89.004(41)	–	–
d' (kHz)	−42.701(78)	−42.54(11)	–	–
δ' (kHz)	−6.943(86)	−7.04(12)	–	–
ΔeQq (MHz)	1908.381(1)[c]	1908.432(1)[c]	–	–
ΔC (kHz)	86.350[c]	86.100[c]	–	–
Δd (kHz)	−44.225[c]	−44.064[c]	–	–
$\Delta\delta$ (kHz)	−10.647[c]	−10.744[c]	–	–

[a] The hyperfine constants of $R(15)43\text{-}0$ and $P(13)43\text{-}0$ are taken from Refs. 21 and 22.
[b] d'' and δ'' in the present fitting are fixed to the values in Refs. 21 and 22.
[c] The uncertainty of the relative values of the hyperfine constants is much smaller than that of the absolute values. For example, the uncertainty of ΔeQq of the $R(56)32\text{-}0$ transition calculated with only main lines is ~1 kHz, whereas the uncertainty of the absolute values of the upper and lower levels is 11 kHz.

2,... if their frequencies are higher than that of a_{10}. It is worth mentioning here that no crossover line was found near a_{10}, a contrary result that would have affected the line shape and the locking condition of the a_{10} component (which is the one used for optical frequency standards).

The hyperfine splittings of both the main and the crossover lines were measured by heterodyne beating of the two iodine-stabilized Nd:YAG lasers. One laser was locked onto a reference line, and the other laser was locked onto those main and crossover lines to be mea-

sured. To reduce the power broadening and the power shift for the main lines, we adjusted the pump (probe) power to ~2.0 (0.4) mW for the main-line measurements.

The measured main and crossover lines of the $R(56)32\text{-}0$ transition are listed in Table 1. For the measurement of main lines, the standard deviation of the beat frequency noise is ~40 Hz, corresponding to ~28-Hz rms noise per laser at 1-s averaging time. The uncertainty of the measured main hyperfine lines, including all the differences between the two spectrometers (iodine cell, modulation frequency, beam size, intensity, etc.), is typically ±300 Hz. A detailed description of the stability and uncertainty of the main-line measurements is given in Ref. 13. For the measurement of crossover lines, the bigger uncertainty arises from the smaller S/N ratio. The corresponding standard deviation of the typical beat frequency noise is ~1 kHz at 1-s averaging time. Some of the crossover lines are not included in the Hamiltonian calculation described in Section 3 below. For example, lines −1 and −2 near a_{10} are excluded because they are too close to each other, and lines 1 and −3 are excluded because their measured standard deviation has exceeded 3 kHz. Crossover line 2, which is included in the calculation, is designated c_{9a}.

The measured main and crossover lines of the $P(54)32\text{-}0$ transition are listed in Table 2. The values of the main line splittings have been published in Ref. 13.

3. CALCULATION OF HYPERFINE SPLITTINGS AND COUPLING CONSTANTS

As described in Section 1, the hyperfine Hamiltonian can be written as

$$H_{\mathrm{hfs}} = eQq \times H_{\mathrm{EQ}} + C \times H_{\mathrm{SR}} + d \times H_{\mathrm{TSS}} + \delta \times H_{\mathrm{SSS}}. \quad (1)$$

The electric quadrupole interaction $eQq \times H_{\mathrm{EQ}}$ and the spin–rotation interaction $C \times H_{\mathrm{SR}}$ were introduced by Kroll[27]; the tensor spin–spin interaction $d \times H_{\mathrm{TSS}}$ was introduced by Bunker and Hanes[28]; the scalar spin–spin interaction $\delta \times H_{\mathrm{SSS}}$ was introduced by Hackel *et al.*[29,30] We follow the procedure outlined by Bordé *et al.*[3] to calculate the eigenstates of the hyperfine Hamiltonian. In calculating the electric quadrupole interactions, we take ΔJ up to ±4 into account. The rotational Hamiltonian H_R,

$$\langle JIF|H_R|JIF\rangle = BJ(J+1) - DJ^2(J+1)^2 + HJ^3(J+1)^3, \quad (3)$$

was introduced in this calculation, where I is the total nuclear spin and F is the total angular momentum. The necessary rotational constants B, D, and H are taken from Ref. 31. As our observed results include both main and crossover lines, not only the differences but also the absolute values of the hyperfine constants of both upper and lower levels can be obtained. In the present calculation, the hyperfine splittings are fitted to the measurements by a least-squares fit, where the hyperfine constants eQq'', eQq', C'', C', d', and δ' are varied. The lower-level hyperfine constants d'' and δ'' are fixed to the values given in Ref. 21 and shown in Table 3. This is reasonable because d'' and δ'' did not show J dependence in Ref. 21, and we could obtain higher fitting accuracy by fixing d'' and δ''. The lower-level hyperfine constant C'' is not fixed in the present calculation, because the observed intervals of the crossover lines could be better reproduced by the least-squares fit when C'' was also varied. A weight of 10 is applied to the measured main lines; a weight of 1 is applied to the measured crossover lines.

The calculated hyperfine splittings, and their differences from the observed values of the $R(56)32\text{-}0$ transition, are listed in Table 1. The standard deviation is ~500 Hz for the fit that includes only main lines. The main lines of the $R(56)32\text{-}0$ transition were also measured and calculated by Arie and Byer.[10] We achieved an uncertainty more than tenfold smaller in both the measured and the fitted results than in the results reported in Ref. 10. Fifteen crossover lines are included in the calculation for the $R(56)32\text{-}0$ transition. The standard deviation of the fit, including both the main and the crossover lines, is ~0.95 kHz. The fitted hyperfine constants for both the upper and the lower levels of the $R(56)32\text{-}0$ transition are listed in Table 3.

For the $P(54)32\text{-}0$ transition, the calculated hyperfine splittings and their differences from the observed values are listed in Table 2. The standard deviation is ~400 Hz for the fit that includes only main lines. Eight crossover lines are included in the calculation for the $P(54)32\text{-}0$ transition. The standard deviation of the fit, including both the main and the crossover lines, is ~1.13 kHz. The fitted hyperfine constants for both the upper and the lower levels of the $P(54)32\text{-}0$ transition are also listed in Table 3.

The uncertainty in the absolute values of the hyperfine constants listed in Table 3 comes mainly from the measurement uncertainty of the crossover lines, which is due to their smaller S/N ratio. The recoil shift of the saturation resonances is not included in the present calculation. A detailed discussion of the intensities and recoil structure of the main components and the crossovers can be found in Ref. 32.

We also list the relative values of the hyperfine constants $\Delta(eQq)$, ΔC, Δd, and $\Delta\delta$ in Table 3. The calculated $\Delta(eQq)$ (=1908.432 MHz) for the $P(54)32\text{-}0$ transition is in complete coincidence with the value [=1908.432(1) MHz] in Ref. 13, where only the main lines have been included. This is to say that at this level of uncertainty (several hundreds of hertz for both the observation and the calculation), the main hyperfine lines can still be well described by the differences in the hyperfine constants. Empirical formulas for $\Delta(eQq)$, ΔC, Δd, and $\Delta\delta$ were discussed in Ref. 33. The calculated $\Delta(eQq)$ [=1908.381(1) MHz] for the $R(56)32\text{-}0$ transition is smaller but more accurate than the value [=1908.406(10) MHz] in Ref. 11.

By combining the calculated ground state $eQq''(J'' = 54, 56)$ with the $eQq''(J'' = 13, 15)$ obtained in Ref. 21, we found a formula for the rotational dependence of eQq''. As listed in Table 3, our calculated eQq'' shows a difference between $J'' = 54$ and $J'' = 56$ that is larger than that of Bordé and co-workers. We list eQq'' values for the $R(15)43\text{-}0$ and $P(13)43\text{-}0$ transitions[21] in Table 3 for comparison. Figure 3 shows the hyperfine constant

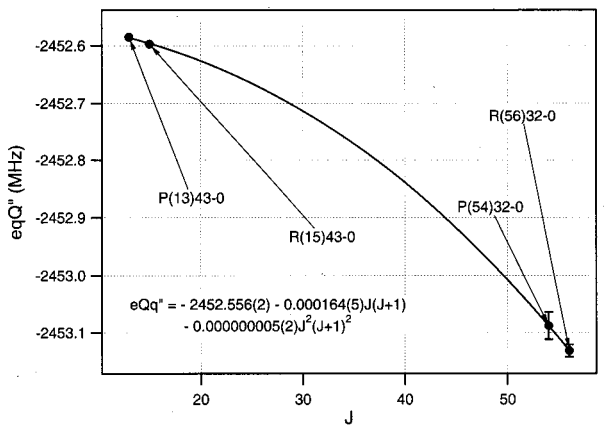

Fig. 3. Ground-state electric quadrupole hyperfine constant eQq'' as a function of rotational quantum number J. Filled circles, eQq'' values calculated from the observed hyperfine splittings. Solid curve, the fitting result for both $J(J+1)$ and $J^2(J+1)^2$ terms. The eQq'' values of $P(13)43\text{-}0$ and $R(15)43\text{-}0$ transitions are taken from Ref. 21.

eQq'' as a function of the rotational quantum number J. We propose the following formula:

$$eQq'' = eQq_0'' + \alpha J(J+1) + \beta J^2(J+1)^2, \quad (4)$$

to express the J dependence of ground state $(v''=0)eQq''$, where eQq_0'' is ground state eQq'' without any vibrational and rotational effects and α and β are the coefficients of the rotational effect. By fitting the calculated eQq'' data to the proposed formula, we obtained

$$eQq_0'' = -2452.556(2)\ \text{MHz}, \quad (5)$$

$$\alpha = -0.164(5)\ \text{kHz}, \quad (6)$$

$$\beta = -0.005(2)\ \text{Hz}. \quad (7)$$

The fitting result is shown in Fig. 3 as a solid curve. We obtained a smaller chi-square value (2.2×10^{-6}) of the fitting, by using the formula including both the $J(J+1)$ and the $J^2(J+1)^2$ terms, than that (8.1×10^{-6}) of the fitting obtained by using the formula including only the $J(J+1)$ term.

The knowledge obtained of the ground-state hyperfine constants is important in metrology, because one can then reliably calculate the influence from neighboring weak transitions on the main lines that may be used for frequency references.

4. DISCUSSION

The obtained rotation dependence of the ground state eQq'' is naturally considered to be associated with the centrifugal distortion effect in the electric quadrupole hyperfine interaction. The centrifugal force changes the distance between the two nuclei in the molecule, which changes the value of the electric field gradient q. A simple analogy exists between the calculation of rotational energy and the present J dependence of eQq''. As shown in the first term of Eq. (3), the rotational energy for a rigid rotor is expressed as

$$E(J) = BJ(J+1). \quad (8)$$

The largest correction for this expression is the centrifugal distortion correction shown in the second term of Eq. (3). Thus the rotational energy with centrifugal distortion correction is expressed as

$$E(J) = BJ(J+1) - DJ^2(J+1)^2. \quad (9)$$

At $J\sim55$, the third term of Eq. (3) is only 0.03% of the D-dependent term. Equation (8) can also be written as

$$E(J) = B'J(J+1), \quad (10)$$

where

$$B' = B - DJ(J+1) \quad (11)$$

is the centrifugal-distortion-corrected rotational constant (and we note that both B and D are positive). Equation (11) is analogous to the first two terms of Eq. (4), which we have proposed to represent the electric quadrupole hyperfine constant.

To illustrate the issue, mechanically we have

$$r_e = \left(\frac{h}{4\pi^2 BM}\right)^{1/2}, \quad (12)$$

where r_e and M are the equilibrium separation and the mass of the iodine nuclei, respectively. Equations (11) and (12) allow us to estimate the change of r_e, Δr_e, with J as

$$\Delta r_e/r_e = {}^1\!/_2(D/B)J(J+1), \quad (13)$$

$\sim+3.7\times10^{-4}$ at $J\sim55$. We note that, on the one hand, our experiment associates an increase in $|eQq|$ with increasing J and r_e, beginning from $|eQq_0| = 2452.556(2)$ MHz for the ground electronic state with $v''=0$ and $J''=0$, as shown in Fig. 3 and Eq. (5). On the other hand, stretching of the molecule with increasing J leads to the separated-atom picture, with the limiting atomic $|eQq_A| = 2292.71$ MHz.[34] This nonmonotonic behavior of $eQq(r_e)$ will be fascinating to explore in the future.

More-detailed theoretical discussions can be found in Refs. 35–37. In general, the magnetic and electric fields inside a molecule depend on the internuclear distances and hence on the vibration-rotation state of the molecule. Any molecular constant associated with a given hyperfine interaction can then be considered a function of the internuclear distance and expressed as a Taylor expansion about the equilibrium position. For a diatomic molecule in the electronic state $^1\Sigma$, the average value in the vibration-rotation state $|vJ\rangle$ of an operator X, a function of internuclear distance r, can be expanded in terms of the relative distance ξ to the equilibrium position r_e (in the present case X is a short notation for eQq):

$$\langle X\rangle_{vJ} = X_e + X_e'\langle\xi\rangle_{vJ} + (1/2)X_e''\langle\xi^2\rangle_{vJ} + \ldots, \quad (14)$$

where $\xi = (R-R_e)/R_e$ and $\langle X\rangle_{vJ} = \langle vJ|X|vJ\rangle$.

The various matrix elements $\langle\xi^n\rangle_{vJ} = \langle vJ|\xi^n|vJ\rangle$ can be expressed as power series in $v+1/2$ and $J(J+1)$:

$$\langle\xi^n\rangle_{vJ} = \sum_{lj} Z_{lj}^{(n)}[v+(1/2)]^l[J(J+1)]^j, \quad (15)$$

where the coefficients $Z_{lj}^{(n)}$ are functions of B_e/ω_e and of Dunham's potential constants a_i.

A calculation of the coefficient $Z_{lj}^{(n)}$ valid to third order in B_e/ω_e was made by Herman and Short.[35] If we limit ourselves to second order in B_e/ω_e,

$$\langle X\rangle_{vJ} = X_e + \frac{B_e}{\omega_e}\left(v + \frac{1}{2}\right)(X_e'' - 3a_1X_e') + \left(v + \frac{1}{2}\right)^2\left(\frac{B_e}{\omega_e}\right)^2 \times \left[X_e'\left(-15a_3 + 39a_1a_2 - \frac{45}{2}a_1^3\right) + \frac{1}{2}X_e''(15a_1^2 - 6a_2) - \frac{15}{6}X_e'''a_1 + \frac{1}{4}X_e''''\right] + 4\left(\frac{B_e}{\omega_e}\right)^2 X_e'J(J+1), \quad (16)$$

in agreement with the formula of de Leeuw and Dymanus[36] and of Watson.[37,38] The last term is of course the interesting one to us because it provides the quantum-mechanical justification of the simple formula derived in the present paper from semiclassical considerations with the *a priori* knowledge that $D_e/B_e = 4(B_e/\omega_e)^2$. As a result, the variation with J of eQq for diatomic molecules is expressed as

$$eQq = eQq_0 + 4(B_e/\omega_e)^2J''(J''+1)(eQq)' + \ldots. \quad (17)$$

At the next order in B_e/ω_e we find a crossed term in $(v + 1/2)J(J+1)$ that has to be considered in the future:

$$2\left(\frac{B_e}{\omega_e}\right)^3[3(8 + 9a_1 + 9a_1^2 - 8a_2)X_e' - 3(1+3a_1)X_e'' + 2X_e''']\left(v + \frac{1}{2}\right)J(J+1). \quad (18)$$

The coefficients $B_e, \omega_e, a_1, a_2, \ldots$ are known from vibration-rotation data.

More interestingly, in the near future a larger number of accurate data will enable one to invert the problem so that one can find the functional dependence of $eQq(r)$ on the nucleus separation for different vibration and rotation states.[37–39] With that information we should be able to start exploration of the molecular bonding characteristics.

The rotational dependence of eQq has also been observed for $^{189}OsO_4$, which is a spherical-topped molecule.[40] The J dependence of eQq was visualized as a parabola and confirmed to be affected predominantly by centrifugal distortion. The vibrational and Coriolis-type contributions to the J dependence were also discussed. In $^{189}OsO_4$, the tetrahedral symmetry of the molecule imposes a null electric field gradient at the osmium location. Hence, as expected, $eQq'' \approx 0$ was obtained for the ground vibrational level with $J = 0$.

With Eqs. (4)–(7) we can calculate eQq'' precisely for all the J levels in the ground state with $v'' = 0$. For $J'' = 57$, eQq'' is calculated to be -2453.153 MHz. ΔeQq for the $R(57)32\text{-}0$ transition was determined[13] to be 1908.381 MHz. Therefore we obtain the upper level eQq' for the $R(57)32\text{-}0$ transition as -544.772 MHz. In Table 4, three calculated eQq' are listed. Rotational dependence is again observed for the upper level eQq', with approximately the same coefficient. In the excited states, the electric field gradient is different from that in the ground states, and the vibration of the molecule may also play a role.

Table 4. Calculated Electric Quadrupole Hyperfine Constants of the *B* state ($v' = 32$)

J'	eQq' (MHz)
53	−544.656
57	−544.751
58	−544.772

Ground state eQq'' of I_2 was previously investigated for $J'' = 0-10$ $(v'' = 1)$ by molecular-beam laser spectroscopy.[41] No rotational dependence was found because of the large measurement uncertainty of eQq'' ($\sim$4.5 MHz). The rotational dependence of eQq'' and ΔeQq was discussed by Špirko and Blabla[42] and by Knöckel *et al.*,[43] respectively; however, knowledge of their values was again limited by measurement uncertainty. With the high-frequency stability of our laser systems that results from the high S/N ratio and narrow linewidth of the observed signal, we have reduced the uncertainty of eQq'' to $\sim$10 kHz.

With the high stability available from our lasers, we can also investigate the characteristics of the laser systems more precisely. For example, in the international comparison of the I_2-stabilized Nd:YAG lasers, the hyperfine splitting was found to vary slightly between two different systems.[18] We believe that the difference in wavefront curvature and the residual amplitude modulation in the phase modulation process are the main contributions to the difference of the hyperfine splittings. Another contribution may come from an influence of recoil splitting. In fact, we did perform another least-squares fit with the measured hyperfine splittings properly modified to reflect the estimated recoil shifts associated with the main lines and the crossovers. Results of calculations with the recoil corrections included indicate that the fit uncertainties remain similar. The variation of eQq'' owing to the recoil correction is negligible, well within the standard deviation of the fit. However, the value of C'' does change, depending on whether the recoil correction is included, with a variation of the order of 2–5 times the fit uncertainty. These issues can be investigated more thoroughly when the stability and reliability of the laser systems are improved further. Also, study of the transitions of lower rotational quantum numbers will offer a more-precise determination of the eQq value owing to the stronger intensities of the crossover transitions. Success in these directions will allow us to achieve an even smaller measurement uncertainty in the hyperfine splittings and to test the validity of the four-term Hamiltonian with higher accuracy.

ACKNOWLEDGMENTS

The research at JILA was supported in part by the U.S. Air Force Office of Scientific Research, the National Sci-

ence Foundation, and the National Institute of Standards and Technology as part of its program of research in precision measurements and advanced frequency standards. F.-L. Hong appreciates support by the National Research Laboratory of Metrology, the Ministry of International Trade and Industry, and the Science and Technology Agency, Japan, for his overseas study. Ch. J. Bordé is especially grateful to his good friend J. L. Hall for the kind invitation to work during summer 1998 in Hall's laboratory at JILA; Bordé thanks Jacques Vigué for many enlightening discussions. Ye's e-mail address is ye@jila.colorado.edu.

*Permanent address, National Research Laboratory of Metrology, Tsukuba, Ibaraki 305-8536, Japan.

**Staff member, Quantum Physics Division, National Institute of Standards and Technology.

†Permanent address, Laboratory for Quantum Optics, East China Normal University, Shanghai, China.

‡Bureau International des Poids et Measures, Sèvres Cedex, France.

¶Permanent address, Laboratoire de Physique des Lasers, Université Paris-Nord, Avenue J.-B. Clément, 93430 Villetaneuse, France.

REFERENCES

1. M. D. Levenson and A. L. Schawlow, "Hyperfine interactions in molecular iodine," Phys. Rev. A **6**, 10–20 (1972).
2. H. J. Foth and F. Spieweck, "Hyperfine Structure of the $R(98)$, 58-1 line of $^{127}I_2$ at 514.5 nm," Chem. Phys. Lett. **65**, 347–352 (1979).
3. Ch. J. Bordé, G. Camy, B. Decomps, J.-P. Descoubes, and J. Vigué, "High precision saturation spectroscopy of $^{127}I_2$ with argon lasers at 5145 Å and 5017 Å. I. Main resonances," J. Phys. (Paris) **42**, 1393–1411 (1981).
4. G. R. Hanes and C. E. Dahlstrom, "Iodine hyperfine structure observed in saturated absorption at 633 nm," Appl. Phys. Lett. **14**, 362–364 (1969).
5. P. Cérez and S. J. Bennett, "Helium–neon laser stabilized by saturated absorption in iodine at 612 nm," Appl. Opt. **18**, 1079–1083 (1979).
6. J.-M. Chartier, S. Fredin-Picard, and L. Robertsson, "Frequency-stabilized 543 nm HeNe laser system: a new candidate for the realization of the meter?" Opt. Commun. **74**, 87–92 (1989).
7. B. Couillaud and A. Ducasse, "Saturated absorption experiments using a free running cw dye laser," Opt. Commun. **13**, 398–401 (1975).
8. A. Razet and S. Picard, "A tabulation of calculations of the hyperfine structure in $^{127}I_2$," Metrologia **33**, 19–27 (1996).
9. J. L. Hall, L.-S. Ma, M. Taubman, B. Tiemann, F.-L. Hong, O. Pfister, and J. Ye, "Stabilization and frequency measurement of the I_2-stabilized Nd:YAG laser," IEEE Trans. Instrum. Meas. **48**, 583–586 (1999).
10. A. Arie and R. L. Byer, "Laser heterodyne spectroscopy of $^{127}I_2$ hyperfine structure near 532 nm," J. Opt. Soc. Am. B **10**, 1990–1997 (1993).
11. A. Arie and R. L. Byer, "The hyperfine structure of the $^{127}I_2$ $P(119)$ 35-0 transition," Opt. Commun. **111**, 253–258 (1994).
12. M. L. Eickhoff and J. L. Hall, "Optical frequency standard at 532 nm," IEEE Trans. Instrum. Meas. **44**, 155–158 (1995).
13. J. Ye, L. Robertsson, S. Picard, L.-S. Ma, and J. L. Hall, "Absolute frequency atlas of molecular I_2 lines at 532 nm," IEEE Trans. Instrum. Meas. **48**, 544–549 (1999).
14. T. J. Quinn, "Practical realization of the definition of the metre (1997)," Metrologia **36**, 211–244 (1999).
15. P. A. Jungner, S. Swartz, M. Eickhoff, J. Ye, J. L. Hall, and S. Waltman, "Absolute frequency of the molecular iodine transition $R(56)32$-0 near 532 nm," IEEE Trans. Instrum. Meas. **44**, 151–154 (1995).
16. P. Jungner, M. L. Eickhoff, S. D. Swartz, J. Ye, and J. L. Hall, "Stability and absolute frequency of molecular iodine transitions near 532 nm," in *Laser Frequency Stabilization and Noise Reduction*, Y. Shevy, ed., Proc. SPIE **2378**, 22–34 (1995).
17. F.-L. Hong, J. Ishikawa, T. H. Yoon, L.-S. Ma, J. Ye, and J. L. Hall, "A portable I_2-stabilized Nd:YAG laser for wavelength standards at 532 nm and 1064 nm," in *Recent Developments in Optical Gauge Block Metrology*, N. Brown and J. E. Decker, eds., Proc. SPIE **3477**, 2–10 (1998).
18. F.-L. Hong, J. Ishikawa, J. Yoda, J. Ye, L.-S. Ma, and J. L. Hall, "Frequency comparison of $^{127}I_2$-stabilized Nd:YAG lasers," IEEE Trans. Instrum. Meas. **48**, 532–536 (1999).
19. M. S. Sorem, T. W. Hänsch, and A. L. Schawlow, "Nuclear quadrupole coupling in the $^1\Sigma_g^+$ and $^3\Pi_{ou}^+$ states of molecular iodine," Chem. Phys. Lett. **17**, 300–302 (1972).
20. A. Yokozeki and J. S. Muenter, "Laser fluorescence state selected and detected molecular beam magnetic resonance in I_2," J. Chem. Phys. **72**, 3796–3804 (1980).
21. J.-P. Wallerand, F. du Burck, B. Mercier, A. N. Goncharov, M. Himbert, and Ch. J. Bordé, "Frequency measurements of hyperfine splittings in ground rovibronic states of I_2 by stimulated resonant Raman spectroscopy," Eur. Phys. J. D **6**, 63–76 (1999).
22. (Personal communication of Ch. J. Bordé with J. L. Hall, 1998.)
23. T. W. Hänsch and B. Couillaud, "Laser frequency stabilization by polarization spectroscopy of a reflecting reference cavity," Opt. Commun. **35**, 441–444 (1980).
24. G. Camy, C. J. Bordé, and M. Ducloy, "Heterodyne saturation spectroscopy through frequency modulation of the saturation beam," Opt. Commun. **41**, 325–330 (1982), especially Refs. 6 and 7 therein.
25. J. H. Shirley, "Modulation transfer processes in optical heterodyne saturation spectroscopy," Opt. Lett. **7**, 537–539 (1982).
26. L. S. Ma, J. H. Shirley, L. Hollberg, and J. L. Hall, "Modulation transfer spectroscopy for stabilizing lasers," U.S. patent 4,590,597 (May 26, 1986).
27. M. Kroll, "Hyperfine structure in the visible molecular-iodine absorption spectrum," Phys. Rev. Lett. **23**, 631–633 (1969).
28. P. R. Bunker and G. R. Hanes, "Nuclear spin-spin coupling in the spectrum of I_2 at 6328 Å," Chem. Phys. Lett. **28**, 377–379 (1974).
29. L. A. Hackel, K. H. Casleton, S. G. Kukolich, and S. Ezekiel, "Observation of magnetic octupole and scalar spin-spin interaction in I_2 using laser spectroscopy," Phys. Rev. Lett. **35**, 568–571 (1975).
30. See also B. M. Landsberg, "Nuclear hyperfine splittings in $B-X$ electronic band system of $^{127}I_2$," Chem. Phys. Lett. **43**, 102–103 (1976).
31. S. Gerstenkorn and P. Luc, "Description of the absorption spectrum of iodine recorded by means of Fourier transform spectroscopy: the $(B-X)$ system," J. Phys. (Paris) **46**, 867–881 (1985).
32. Ch. J. Bordé, G. Camy, N. and B. Decomps, "Measurement of the recoil shift of saturation resonances of $^{127}I_2$ at 5145 Å: a test of accuracy for high-resolution spectroscopy," Phys. Rev. A **20**, 254–268 (1979). J. Bordeé and Ch. J. Bordé, "Intensities of hyperfine components in saturation spectroscopy," J. Mol. Spectrosc. **78**, 353–378 (1979).
33. A. Razet and S. Picard, "A test of new empirical formulas for the prediction of hyperfine component frequencies in $^{127}I_2$," Metrologia **34**, 181–186 (1997).
34. V. Jaccarino, J. G. King, R. A. Satten, and H. H. Stroke, "Hyperfine structure of I^{127}. Nuclear magnetic octupole moment," Phys. Rev. **94**, 1798–1616 (1954).

35. R. M. Herman and S. Short, "New theoretical method for the accurate calculation of expectation values on functions of internuclear in $^1\Sigma$-state diatomic molecules," J. Chem. Phys. **48**, 1266–1272 (1968).
36. F. H. de Leeuw and A. Dymanus, "Magnetic properties and molecular quadrupole moment of HF and HCl by molecular-beam electric-resonance spectroscopy," J. Mol. Spectrosc. **48**, 427–445 (1973).
37. J. K. G. Watson, "The inversion of diatomic vibration-rotation expectation values," J. Mol. Spectrosc. **74**, 319–321 (1979).
38. See also P. R. Bunker, "The breakdown of the Born–Oppenheimer approximation for a diatomic molecule: the dipole moment and nuclear quadrupole coupling constants," J. Mol. Spectrosc. **45**, 151–158 (1973).
39. G. Gouédard, N. Billy, B. Girard, and J. Vigué, "Hyperfine structure measurements in the IF $B-X$ system," J. Phys. II **2**, 813–825 (1992).
40. Ch. Chardonnet, M. L. Palma, and Ch. J. Bordé, "Hyperfine interactions in the v_3 band of osmium tetroxide: the electric quadrupole interaction in $^{189}OsO_4$," J. Mol. Spectrosc. **170**, 542–566 (1995).
41. M. Wakasugi, T. Horiguchi, M. Koizumi, and Y. Yoshizawa, "Hyperfine structure near the 13-1 band head in the $B-X$ transition of $^{127}I_2$," J. Opt. Soc. Am. B **5**, 2298–2304 (1988).
42. V. Špirko and J. Blabla, "Nuclear quadrupole coupling functions of the $^1\Sigma_g^+$ and $^3\Pi_{0u}^+$ states of molecular iodine," J. Mol. Spectrosc. **129**, 59–71 (1988).
43. H. Knöckel, S. Kremser, B. Bodermann, and E. Tiemann, "High precision measurement of hyperfine structures near 790 nm of I_2," Z. Phys. D **37**, 43–48 (1996).